Charm Production at HERA and at Hadron Colliders

Martin zur Nedden[1]
[1]Humboldt-Universität zu Berlin, Germany

Experimental results of open charm and charmonium production at HERA and TEVATRON are reviewed within this article giving an outlook to LHC. The charm contribution to the proton structure function, the charm fragmentation function and the production of charmonium states in media measured at HERA are discussed. Some selected topics concerning as associates W and charm jets and flavour changing neutral curents from TEVATRON are shown and an outlook to charmonium measurements at LHC is given.

Introduction

Charm production at HERA and TEVATRON is a very rich field, which can only be covered partially here. With respect to the upcoming data from LHC, the focus will be set on the charm contribution to the proton structure function, charm fragmentation functions and production of chamonium in hadronic interaction as measured at HERA. The studies of associated production of W-bosons with charm-jet and flavour changing neutral currents at TEVATRON are important measurement to understand the background for the search for new physics beyond the standard model at LHC. The production of charmonium states in media is discussed as well since an understanding of the basic mechanisms responsible for the suppression of charmonium production in proton-nucleus collisions relative to proton-nucleon collisions is a prerequisite for the identification of possible signals of new physics in high-energy heavy-ion data as expected at LHC.

After a short discussion of the production mechanism of heavy flavours in hadronic and electron-proton interaction, the measurements of the charm contribution to the proton structure function and the charm fragmentation function from HERA are shown, followed by the charmonium spectroscopy and production in media done with HERA-B. After two examples form TEVATRON, the measurement of the associated $W+$ charm-jets and the search for flavour changing neutral currents, an outlook to the expected data from LHC is given including the perspectives for a measurement of the J/ψ polarization in hadrondic interactions.

Production of Heavy Quarks

The production of heavy flavours in hadronic interactions at TEVATRON and LHC is shown in Fig. 1, which are also valid for the proton-fixed target interactions at HERA-B (Fig. 3). The heavy quark pair can be produced by leading order flavour creation, flavour excitation (NLO) and gluon splitting (NLO). Hadrons with open or hidden charm and c-flavoured jets, which are the observables of the charm-quarks, are the produced based on the fragmentation function $D^{c\to c-\mathrm{hadron}}$, which has to be extracted form experimental data (see Sec.).

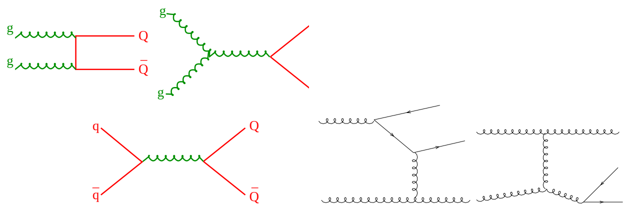

Figure 1: Production of heavy flavours at tree levle in hadronic collisions in LO and NLO, flavour excitation and gluon splittig.

In electron proton interactions at HERA (Experiments H1 and ZEUS), heavy flavours can be produced either in direct processes with boson gluon fusion or at indirect processes via a resolved photon or flavour excitation (Fig. 2). Two kinematical regions are discriminated, the photo production region at a momentum transfer of $Q^2 \approx 0$ GeV^2 and the deep inelastic scattering at $Q^2 > 2$ GeV^2. The production of open charm is mainly used at HERA to determine the charm contribution to the proton structure function and the charm fragmentation function. Since the proton sturcture functions are universal, both measurements are important prerequisites for the interpretation of the results of LHC and TEVATRON.

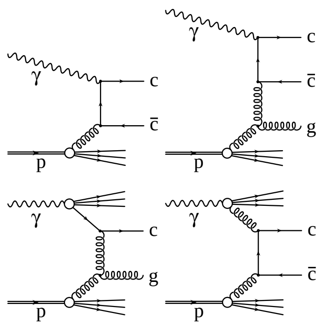

Figure 2: Production of heavy flavours at HERA in direct boson-gluon fusion processes (upper line), via a resolved photon (lower line left) or flavour excitation (lower line right).

Quarkonia Formation

In Eq. 1 the hadronization and fragmentation process shown in Fig. 3 of a final state with charm in hadronic production is described. The process to obtain a charmed

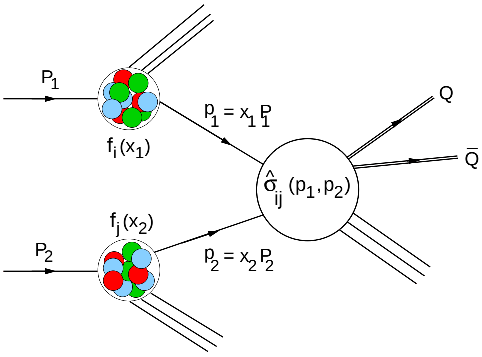

Figure 3: Schematic picture of two colliding nucleons with momentum P_1 and P_2. Two partons inside the nucleons, with momentum fraction x_1 and x_2, interact to create the final state with a heavy quark pair $Q\overline{Q}$.

hadron $\mathcal{CH}$ in the final state can be factorized in three different parts. The first part at an energy scale of $\Lambda_{\rm QCD}$ describes the parton density functions $f_{i/A}$ and $f_{j/B}$ within the hadrons to be measured by other experiments. The second part contains the partonic heavy flavour production cross section, which is a short distance process ($1/m_c$) and can be described within perturbative calculations.

$$\begin{aligned} \sigma_{\mathcal{CH}} &= \sum_{i,j} \int \underbrace{\mathrm{d}x_1\,\mathrm{d}x_2\, f_{i/A} f_{j/B}}_{\Lambda_{\rm QCD}} \\ &\times \underbrace{\hat{\sigma}\Big(ij \rightarrow (c\bar{c}[n] + X')\Big)}_{m_c} \\ &\times \underbrace{\mathcal{O}[c\bar{c} \rightarrow \mathcal{CH}]}_{m_c v} + \mathcal{O}\Big(\frac{\Lambda_{\rm QCD}}{m_c^2}\Big) \qquad (1) \end{aligned}$$

Finally in the third part, the quarkonia formation process after the production of heavy flavours in a hadronic interaction requires an colour neutral final state and is a long distance process ($1/(m_c v)$) where non-perturbative calculation and inputs form other experiments are needed. By a simple gluon fusion, a colour-neutral $J^P = 1^-$ state can not be produced. This can be achieved by the radiation of a single hard gluon in the Color Single Model (CSM) or by the radiation of many soft gluon (Color Octet Model, based on non relativistic QCD). Whereas the CSM underestimates the cross sections by a factor of 10 - 50 and the p_T-spectrum does not match the data, the COM has adjustable hadronization parameters to match the cross section and kinematical distributions and polarization effects can be described. Measuring various charmonium final states produced in hadronic interaction by doing spectroscopy is one of the main tools to dicriminate between different charmonium formation models. The formation process of quarkonia within media has to be known well in order to interpret the expected data at heavy ion collisions at LHC.

HERA

In the first section, some highlights form HERA are presented. The experiments H1 and ZEUS could collect an integrated luminosity of $0.5\ \mathrm{fb}^{-1}$ per experiment of electron proton collisions at $\sqrt{s} = 320$ GeV. Since the finishing of HERA in 2007 common analyses of H1 and ZEUS data could be carried out at high precision. The HERA-B experiment was able to reconstruct in proton fixed target interaction at $\sqrt{s} = 42$ GeV about 300.000 J/ψ's, 15.000 χ_c's and 5.000 ψ''s. The main topics of the HERA-experiments were:

- differential cross sections of charm production
- charm contribution to F_2 (H1, ZEUS)
- charm fragmentation function D^c (H1, ZEUS)
- charmonium spectroscopy (H1, ZEUS and HERA-B)
- excited charmed states (H1, ZEUS and HERA-B)
- charm production in media (HERA-B only)

Charm Contribution to Proton Structure function

The measurements of the charm contribution $F_2^{c\bar{c}}$ to the proton structure function F_2 at HERA is an important test QCD constraining the parton density functions PDFs of the proton. Precise knowledge of the PDFs of the proton is essential for the interpretation of the measurements at the LHC. The predictions of the so called 'standard candle' QCD process at the LHC, auch as the inclusive production of W and Z bosons, are sensitive to the theoretical treatment of heavy flavours. The data provided by the experiments H1 and ZEUS show a clear evidence that the dynamics of charm production in ep scattering is dominated by the photon gluon fusion process. The available data cover a range of photon virtuality of $2 < Q^2 < 1000\ \mathrm{GeV}^2$ and Bjorken scaling variable $10^{-5} < x < 10^{-1}$. In this framework, the process $e^+p \rightarrow e^+c\bar{c}X$ is sensitive to the gluon density in the proton and allows to tests its universality. The analysis presented here uses published and preliminary data from H1 (387 pb^{-1} of integrated luminosity, [1]) and ZEUS (379 pb^{-1} of integrated luminosity, [2]) collected in the HERA-I and and HERA-II running periods.

The D meson production cross section measured in a given bin of x and Q^2 and in the visible phase space defined by the cuts on η and p_T on the D-meson are transformed to $F_2^{c\bar{c}}$ at a reference x, Q^2 point at

$$F_2^{c,\mathrm{meas}}(x,Q^2) = \sigma^{\mathrm{meas}}_{\mathrm{vis,bin}} \cdot \frac{F_2^{c,\mathrm{model}}(x,Q^2)}{\sigma^{\mathrm{model}}_{\mathrm{vis,bin}}} \qquad (2)$$

using NLO calculation at FFNS [3]. The averaged $F^{c\bar{c}_2}$ of H1 and ZEUS is obtained combining the D-meson measurements and the results of the displaced track and semi-leptonic decay analyses. The results are compared to perturbative QCD approaches.

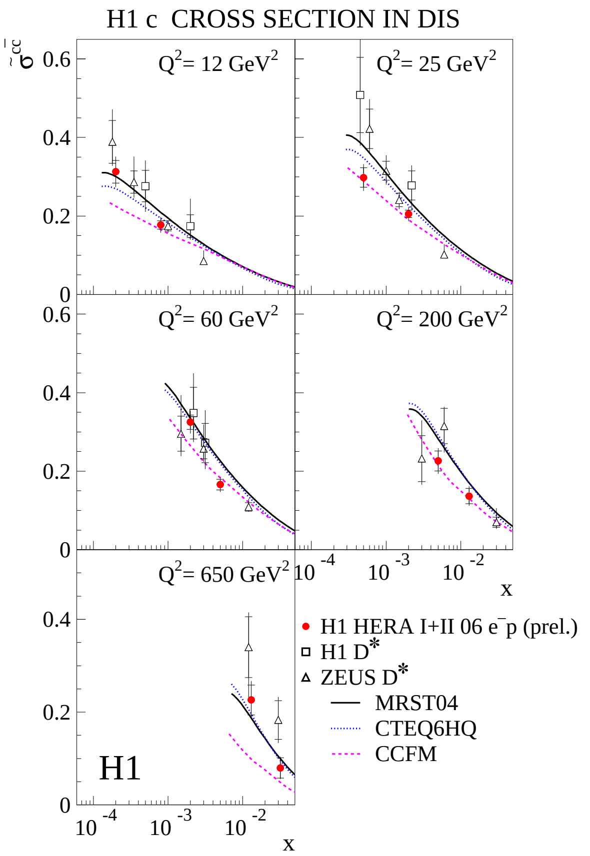

Figure 4: D^* differentail cross section measurement as a function of x in bins Q^2. The results from H1 and ZEUS are shown compared to recent QCD NLO calculations.

In Fig. 4 the D^* differential cross sections are shown in bins of x and Q^2 and can be described reasonable by NLO QCD calculations. The double differential cross sections in x and Q^2 are the basis for the extraction of $F_2^{c\bar{c}}$ as shown in Fig. 5, where the comparision of the data with the recent theory calculation are shown. The combination of the the H1 and ZEUS data uses a χ^2 minimization mehtod taking into account the correlated systematic uncertaintis for the H1 and ZEUS cross section measurements [5].

Charm Fragmentation Function

The process of charm quark fragmentation is studied using $D^{*\pm}$ meson production in deep inelastic scattering to investigate the transition of a charm quark into a meson. However, the transition of an on-shell charm quark is not calculable within the framework of perturbative QCD and is described by phenomenological models. One of the characteristics of this transition is the longitudinal

The fragmentation can be studied by measuring the differential production cross section of a heavy hadron as a function of a scaled momentum energy. Since in ep collisions only a fraction of the available E_{cms} contributes to the production of charm quarks in the hard scattering process but charm quarks are produced in the hard scatter form final-state jets of which the meson is a constituent, the fragmentation variable z is calculated as

$$z = \frac{(E + p_{\|})^{D^*}}{2 \cdot E^{\text{jet}}} \tag{3}$$

For the analysis presented here, the parametrization suggested by Peterson

$$D_c^{D^*}(z) \propto \frac{1}{z\left(1 - \frac{1}{z} - \frac{\epsilon}{1-z}\right)^2} \tag{4}$$

and Kartvelishvili:

$$D_c^{D^*}(z) \propto z^\alpha(1 - z) \tag{5}$$

are used, which both depend only on one single free parameter z. The measurements of the differential distributions of z by H1 [6] and ZEUS [7] are both well described by NLO QCD calculation for both parametrization with $\epsilon_{\text{Peterson}} = 0.079^{+0.013}_{-0.009}$ and $\alpha_{\text{Kartvelishvili}} = 2.67^{+0.25}_{-0.31}$, where a jet energy for k_T jets of $E_T^{\text{jet}} > 9$ GeV was required. As can be seen in Fig. 6 the shape measurement of the charm fragmentation function is in good agreement to other experiments. Making use of PYTHIA the phase space was extrapolated to $p_T(D^*) = 0$ and finite bin size a mean value of $\langle z\rangle 0.565 \pm 0.024_{\text{stat}} \pm 0.028_{\text{sys}}$ could be extracted.

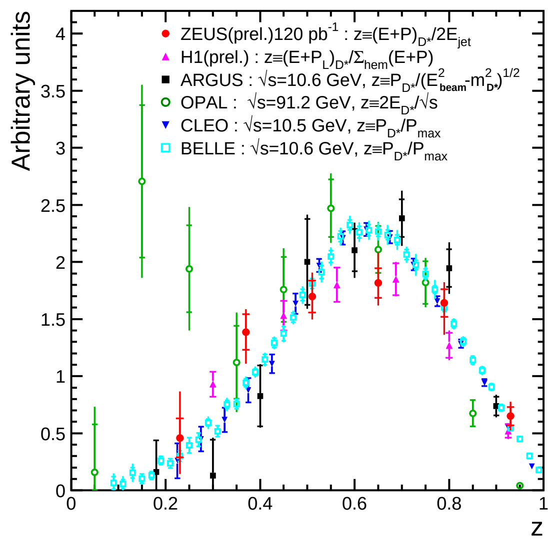

Figure 6: Tjh charm Fragmentation function as a function of z for ZEUS and H1 data compared to measurement of other experiments. For shapre comparision, the data sets are normalized to 1/(bin width) for $z > 0.3$.

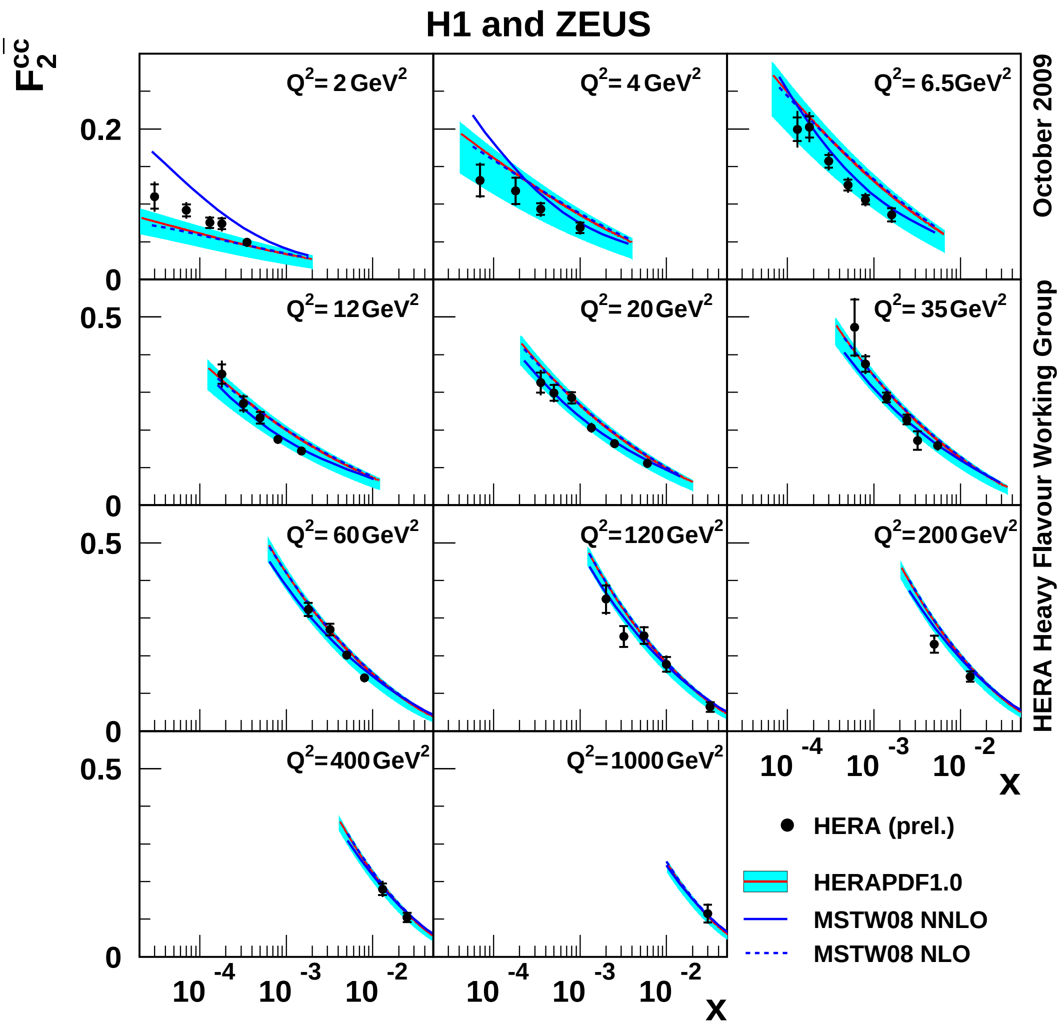

Figure 5: The HERA averaged (combined H1 and ZEUS measurements) $F_2^{\bar{c}c}$-structure function as a function of x in Q^2 bins, compared to recenct QCD predictions at NLO and NNLO (MSTW08 [4].

Charmonium Production in Media

HERA-B is a fixed-target multi-particle spectrometer experiment at the 920 GeV HERA proton beam at DESY. Approximately 150 million events were recorded with a dilepton trigger during the 2002/2003 HERA run. About 300,000 leptonic $J/\psi \rightarrow l^+l^-$ decays (170,000 in the $\mu^+\mu^-$ channel and 130,000 in the e^+e^- channel) have been reconstructed in this data sample. In addition, a huge sample of 220 million minimum biased triggered events were recorded, allowing an independent measurement of the J/ψ production cross section.

The dilepton triggered samples allowed to study the charmonium production in the so far unexplored negative Feynman-x (x_F) region, and will provide an important input for testing the charmonium production mechanism giving access to nuclear dependence of charmonium production, on J/ψ, χ_c and ψ' production and on their differential distributions.

The target wires, close to the 920 GeV proton beam of HERA, are made of different materials (Carbon, Tungsten or Titanium) which can be used simultaneously to perform measurements of the dependence on the atomic mass number A and to control systematic effects. This enables a measurement of the nuclear dependence of the J/ψ-production by using two wires of different materials in parallel. In order to minimize the sensitivity to systematic effects from luminosity and Monte Carlo (MC) efficiency determination, all cross section measurements are performed relative to the J/ψ production cross section. To determine the reference value of $\sigma_{pN}(J/\psi)$ at the HERA-B energy, a global analysis has been performed on all available published J/ψ cross section measurements including the measurement of HERA-B using a sample of $2.3 \cdot 10^8$ minimum bias triggered events, which are independent from the J/ψ triggered data [15]. The best value, obtained from a fit on

$\sigma_{J/\psi}(\sqrt{s})$ with the help of a non relativistic QCD inspired model including color octet, is for the energy of HERA–B of $\sqrt{s} = 41.6$ GeV

$$\sigma_{J/\psi} \quad = \quad (502 \pm 44)\,\text{nb/nucl.} \qquad (6)$$

The $\sigma_{J/\psi}$ value, which is in pretty good agreement to the other experiments, has been used for all further analysis as reference cross section.

A good understanding of the kinematical distributions of J/ψ and ψ' production as a function of x_F and p_T^2 is the basis for further measurements and interpretations of all effects causing nuclear dependence of charmonium production in nuclear interactions. With respect to the earlier experiments in that field, HERA-B is the first fixed target experiment covering the region of negative Feynmann-x ($x_F = \frac{p_L^{\rm cms}}{(p_L^{\rm cms})_{\rm max}}$) in the range of $x_F \in [-0.35, 0.15]$. The negative x_F region corresponds to small forward momenta of the produced $c\bar{c}$ pair leading to a formation of the J/ψ inside the nucleus. Since the p_T coverage of the older experiments is mostly overlapping with HERA-B, a good opportunity for cross checks is given.

The kinematical distributions of the J/ψ production measured at HERA-B [16] are parametrized by the following interpolating functions:

$$\frac{dN}{dp_T} \quad \propto \quad p_T\left(1 + \frac{1}{\beta - 2}\,\frac{p_T^2}{\langle p_T^2\rangle}\right)^{-\beta}, \qquad (7)$$

$$\frac{dN}{dx_F} \quad \propto \quad \exp\left[-\ln 2\left|\frac{x_F - \Delta x_F}{w_{x_F}}\right|^{\gamma}\right]. \qquad (8)$$

and presented in Fig. 7 for p_T and Fig. 8 for x_F. The parameters $\langle p_T^2\rangle$, β, w_{x_F} (width at half maximum), Δx_F (shift of the center of the distribution with respect to $x_F = 0$) and γ are left free in the fit of the distributions. Among the parameters adopted for the description of the data, the width of the p_T distribution ($\langle p_T^2\rangle$), the position of the maximum of the x_F distribution (Δx_F) and, possibly but less significantly, its width (w_{x_F}) show a trend with the mass number A.

The average p_T^2 of particles produced in nuclear collisions increases with the mass of the target nucleus. This "p_T-broadening" effect is commonly explained as a consequence of multiple elastic scattering of the incoming beam parton in the surrounding nucleus before the hard scattering process takes place. The measured increase of $\langle p_T^2\rangle$ with A is shown in Fig. 7 together with the results of experiments at lower energies. The variable of the abscissa, $A^{1/3} - 1$, is approximately proportional to the radius of the target nucleus (i.e. to the average path length of the parton inside the nucleus), with the shift of -1 such that the magnitude of the effect is measured with respect to $A = 1$.

Furthermore, HERA-B observes a difference in shape between the x_F distributions of the J/ψ for different target nuclei consisting of an increasing displacement of the center of the distribution towards negative values. As shown in Fig. 8, J/ψs are produced in tungsten with an x_F distribution which has equal or slightly greater width with respect

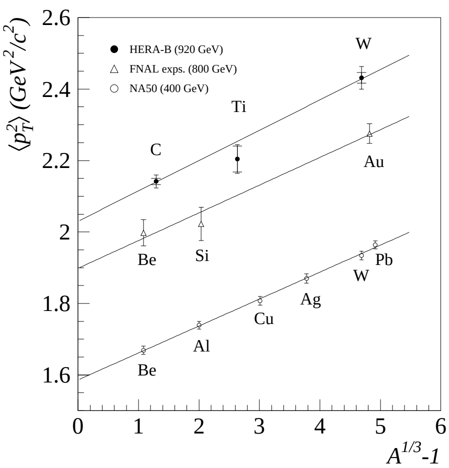

Figure 7: The $\langle p_T^2\rangle$ of the produced J/ψs as a function of $A^{1/3} - 1$ (see Eq. 7). The results of the present analysis (black filled circles with total and statistical uncertainties) are compared to previous measurements performed with different beam energies at Fermilab [17] and at the SPS [10]. The data are fitted with linear functions.

to those produced in carbon and tends to be asymmetrically centered at a lower value. As a possible interpretation, the effect may be attributed to the energy loss undergone by the incident parton and/or the produced state in their path through the nucleus, causing a reduction of the average x_F of the J/ψ – and in addition, possibly, a smearing of the momentum distribution. This hypothesis motivates the choice of representing the data also in this case as a function of $A^{1/3} - 1$.

The Glauber Model [18] suggests that the dependence of the J/ψ production cross section on atomic mass number (A) can be approximated by a power law:

$$\sigma_{pA} = \sigma_{pN} \cdot A^{\alpha}\ , \qquad (9)$$

where σ_{pN} is the proton-nucleon cross section and α, the "suppression" parameter, characterizes the nuclear dependence. Pure hard scattering in the absence of any nuclear effects would correspond to α equal to unity. A suppression of J/ψ production would lead to $\alpha < 1$ while an enhancement (anti-screening effect) would be signaled by $\alpha > 1$. Usually, α is described and measured as a function of x_F and p_T.

The nuclear dependence of the J/ψ production can be measured with low systematic uncertainty by using two different targets with different materials (carbon and tungsten) simultaneously:

$$\sigma \quad (pA \rightarrow J/\psi X) = A^{\alpha} \cdot \sigma(pN \rightarrow J/\psi X)$$
$$\Rightarrow \quad \alpha = \frac{1}{\ln(A_{\rm W}/A_{\rm C})} \cdot \ln\left(\frac{N_{\rm W}^{J/\psi} \cdot \mathcal{L}_{\rm C} \cdot \epsilon_{\rm C}}{N_{\rm C}^{J/\psi} \cdot \mathcal{L}_{\rm W} \cdot \epsilon_{\rm W}}\right) \quad (10)$$

A dependence of the J/ψ production by nuclear effect leads to $\alpha \neq 1$. The measurement making use of the muon

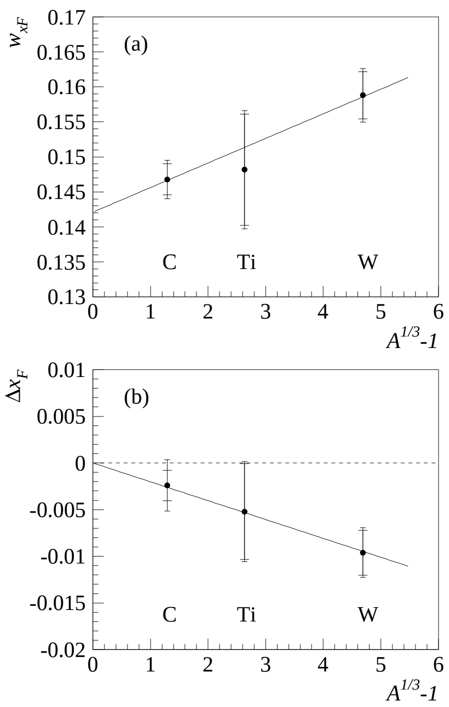

Figure 8: The width (a) and shift (b) of the J/ψ x_F distributions as a function of $A^{1/3} - 1$ (see Eqs. 8). The double error bars represent total and statistical uncertainties. The data are fitted with linear functions.

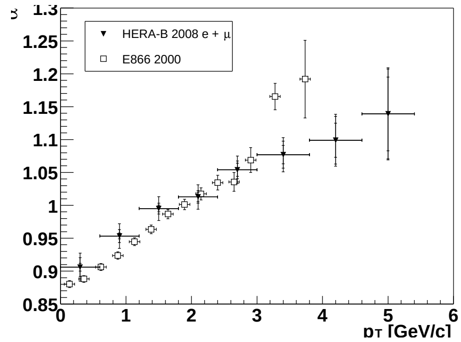

Figure 9: The nuclear suppression parameter α as a function of p_T measured by HERA-B (filled triangles, plotted with total and statistical uncertainties) and by E866 [9] (empty squares).

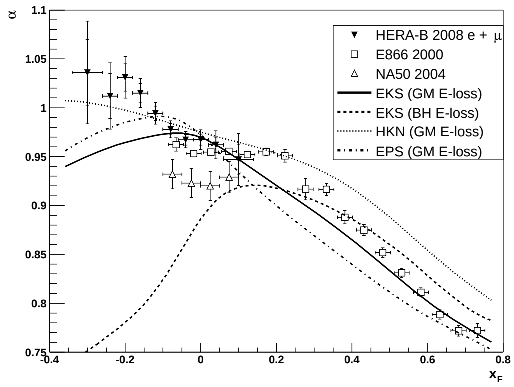

Figure 10: The parameter α describing the nuclear dependence of J/ψ production as a function of x_F measured by HERA-B (filled triangles, plotted with total and statistical uncertainties), by E866 ($\sqrt{s} = 38.8\,\mathrm{GeV}$) [9] (empty squares) and NA50 ($\sqrt{s} = 29.0\,\mathrm{GeV}$) [10] (empty triangles) together with curves from models [8] based on various nuclear parton distributions for $\sqrt{s} = 41.6\,\mathrm{GeV}$ (HERA-B CMS-energy) (EPS [19], EKS [12, 13] and HKN [11]) and initial state energy-loss models [14]. For all approaches, energy loss, intrinsic charm and shadowing are taken into account.

data of HERA-B is compatible with a small suppression with $\alpha = 0.969 \pm 0.003_{\mathrm{stat}} \pm 0.021_{\mathrm{sys}}$ (Fig. 10). This is in good agreement with the theoretical predictions and the earlier measurements in the positive x_F region of the E866 and NA50 experiments (all references are given in [16]. In the commonly covered $x_F$region, a good agreement is found and confirmed by the $\alpha(p_T)$ distribution.

The dependence of J/ψ production in hadron-nucleus interactions on x_F has been modeled by Vogt [8]. Nuclear effects caused by final-state absorption, interactions with co-movers, shadowing of parton distributions, energy loss and intrinsic charm quark components are described separately and integrated into the model. It is further assumed that the $c\bar{c}$ pair is subject to more severe energy losses if produced in a color octet state. Four curves from this model which differ in their descriptions of nuclear Parton Density Functions (nPDF) and energy loss are shown in Fig. 10.

Initial state energy loss as described by Gavin and Milana (GM) and modified by Brodsky and Hoyer (BH) [14], is based on a multiple scattering approach that essentially depletes the projectile parton momentum fraction as the parton moves through the nucleus. Both quarks and gluons can scatter elastically and therefore lose energy before the hard process resulting in an effective reduction of J/ψ production for $x_F > 0$.

The measurement of HERA-B shows that α increases with decreasing x_F and suggests enhanced J/ψ production for $x_F < -0.1$. The HERA-B data favors the nPDFs of EPS and HKN over EKS. The BH description of energy loss is clearly ruled out. None of the variants of the Vogt model give a satisfactory description of both HERA-B and E866 data. For example, while the HKN curve is compatible with most of the HERA-B data points at negative x_F, it lies significantly above the E866 points and furthermore fails to adequately describe RHIC data [19].

A measurement of the production ratio of χ_c to the J/ψ production is an other important tool to discriminate between different models for quarkonium production. HERA-B [20] has access to these states via the radiative decay channel $\chi_c \rightarrow J/\psi\gamma \rightarrow l^+l^-\gamma$ by selecting the χ_c based on the mass difference $\Delta M = M(l^+l^-\gamma) - M(l^+l^-)$. The background is determined by event mixing and subtracted from the spectrum. Using a signal description consisting of two Gaussian and making use of the full statistics' the two states χ_{c_1} and χ_{c_2} can be separated in the applying a rather strong cut on the transverse photon energy of $E_T(\gamma) > 0.4$ GeV.

The production ratio is given as

$$R_{\chi_c} = \frac{\sum_{i=1}^{2} \sigma(pA \to \chi_{c,i}) \cdot BR(\chi_{c,i} \to J/\psi\gamma)}{\sigma(pA \to J/\psi)} = \frac{N_{\chi_c}}{N_{J/\psi}} \cdot \frac{\epsilon_{J/\psi}}{\epsilon_{\chi_c}} \cdot \frac{1}{\epsilon_\gamma} \quad (11)$$

and has been measured to be $R_{\chi_c} = 0.188^{+0.028}_{0.026}$ making use of the independent measurement of the J/ψ reference production cross section based on the minimum bias data sample of HERA-B (Eq. 6. This ratio can be used to test various QCD models for charmonium formation. Since the two χ_{c1} and χ_{c2} states could be disentangled, also their production cross section and the ratio could be measured in the full range of $x_F^{J/\psi}$:

$$\sigma(\chi_{c1}) = (133 \pm 35)\ \text{nb/nucleon}$$
$$\sigma(\chi_{c2}) = (231 \pm 61)\ \text{nb/nucleon} \quad (12)$$

By separately counting the contribution of χ_{c1} and χ_{c2}, a ratio of the two states $R_{12} = R_{\chi_{c1}}/R_{\chi_{c2}} = 1.02 \pm 0.40$ and a cross section ratio of $\frac{\sigma(\chi_{c1})}{\sigma(\chi_{c2})} = 0.57 \pm 0.23$ could be obtained. No significant departure from a flat dependence of R_{χ_c} on the kinematic variables $x_F^{J/\psi}$ and $p_T^{J/\psi}$ is found within the limited accuracy of the measurement of HERA-B. No significant difference in the A-dependence within the limits of the available statistics has been found either for the χ_c states.

TEVATRON

At the TEVATRON collisions of protons and anti-protons at a center of mass energy of $\sqrt{1.8}$ TeV up to $\sqrt{1.96}$ TeV are provided. The two multi purpose detectors, CDF and D0, could collect a total luminosity of ≈ 3 fb^{-1} per experiment so far. Even if the main focus of the physics analysis of the $p\bar{p}$ collision lays within the field of top physics and the searches for the Higgs boson and new phenomena beyond the Standard Model, many exciting topics with in charm physics could be covered:

- D^0-mixing and CP violation
- excited charmed states
- Flavour Changing Neutral Currents
- charmonium fragmentation
- W+charmed jets
- charmonium spectroscopy and polarization

W with associated charmed jets

The associated production of a W-boson and a charmed jet is a possible background to top-quark production and the search for the supersymmetric charged Higgs and the supersymetric $\tilde{t}$-quark. Since the CKM-matrix element $|V_{cd}|^2$ suppressed the d-quark-gluon fusion production, the $W+c-$ jet production is a directly sensitive to the s-quark parton density functions within the proton in the process $p\bar{p}/pp \to s + g \to W^-$. With respect to the possible process $p\bar{p}/pp \to s\bar{c} \to H^-$ this measurement is important for the searches for super symmetric effects at TEVATRON and LHC. Additionally, this is a probe of the s-quark PDF in hadronic interactions probing the QCD.

A measurement of the $W + c -$ jet fraction has been performed by the CDF and D0 collaborations based on an integrated luminosity of ≈ 1.8 fb^{-1} To describe the Standard Model expectation, ALPGEN was used to calculate the matrix elements and PYTHIA to do the showering and hadronization. A measurement of the cross section fraction of $\sigma(W + c - \text{jet})$

$$R = \frac{\sigma(p\bar{p} \to W + c - \text{jet})}{\sigma(p\bar{p} \to \text{jets})} = 0.071 \pm 0.017 \quad (13)$$

was performed by the D0 [22] experiment with ≈ 1.0 fb^{-1} of luminosity and found in good agreement with the theory prediction as a function of the pT of the jet. All leptonic decay channels of the W were considered and the $Z \to \mu^+\mu^-$ background was rejected by requiring $M_{\mu\mu} < 70$ GeV for the μ-channel.

The total cross section of the the associated $W + c -$ jet production was measured by the CDF collaboration based on a luminosity of 1.8 fb^{-1} [21] considering both, the e and μ decay channel of the W boson decay. The charmed jet was identified form the semi leptonic decay by looking for a muon within the jet requiring $p_T^\mu > 3$ GeV$/c$ and ΔR(jet $-$ axis < 0.6. For a clean signal, additionally $p_T(c - \text{jet}) > 20$ GeV$/c$ and $|\eta(c - \text{jet})| < 1.5$ was required. The measured cross section of $\sigma_{W+c-\text{jet}} \times BR(W \to l\nu) = 9.8 \pm 2.8(\text{stat.})^{+1.4}_{-1.6}\,(\text{sys.}) \pm 0.6(\text{lumi})$ pb is in good agreement with the standard model theory prediction of $\sigma^{\text{SM}}_{W+c-\text{jet}} = 11.0^{+1.4}_{-3.0}$ pb. In Fig. 11 the p_T distribution in two kinematical regions are shown for muons, where the background of the same sing di-muon pairs is subtracted. The distribution shows both, the expected $W + c -$ jet signal and the estimated background. Within the quoted sensitivity, no evidence of the presence of an exotic particle with high semileptonic BR could be seen.

Flavour changing neutral currents

The HERA-B [23] and the CDF [24] collaborations have performed a search for flavour chaining neutral currents in the decay $D^0 \to \mu^+\mu^-$ which are forbidden in the standard model at tree level. They can only be realized via penguin or box diagrams and are therefore strongly suppressed leading to a predicted branching ratio of $BR(D^0 \to \mu^+\mu^-) \approx$

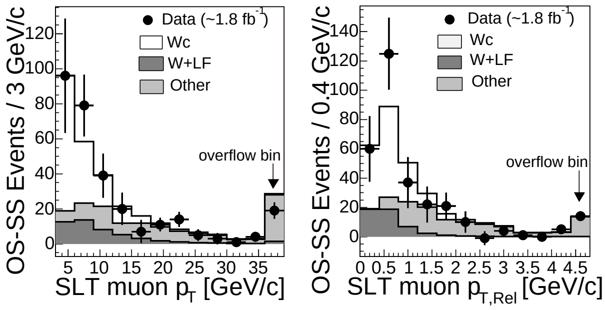

Figure 11: The same sing subtracted distribution of the muon p_T relative to the beam axis (a) and the the jet axis. The $W + c - \mathrm{jet}$ contribution is normalized to this measurement

$3 \cdot 10^{-13}$ within the standard model. This branching ratio would be enhanced in the case of the presence of processes beyond the standard model, in the example of R-parity violating SUSY process a branching ratio of $BR(D^0 \rightarrow \mu^+\mu^-) \approx 3.5 \cdot 10^{-6}$ could be expected.

In Fig. 12 the CDF measurements making use of $69\ \mathrm{pb}^{-1}$. In order to cancel acceptance effects the measurement war normalized to the process $D^0 \rightarrow \pi^+\pi^-$. Also the HERA-B experiment was able to do the same measurement based on the events triggered by the di-muon trigger. Both results at $90\ \%$ confidence level of

$$\begin{aligned} BR(D^0 \rightarrow \mu^+\mu^-) &< 2.0 \cdot 10^{-6}\ (\mathrm{HERA-B}) \\ BR(D^0 \rightarrow \mu^+\mu^-) &< 2.4 \cdot 10^{-6}\ (\mathrm{CDF}) \end{aligned} \quad (14)$$

are compatible and clearly disfavor the strong R-parity violating SUSY processes mentioned above. This results could be used to constrain the R-parity violating couplings

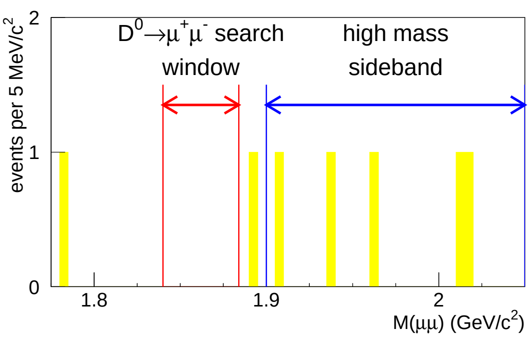

Figure 12: Flavour changing neutral currents form CDF

Outlook to LHC

Even if the focus of the LHC physics is not in the region of charm production, there are nevertheless many topics, which are especially important during the start up phase of the LHC:

- charmonium spectroscopy
- charmonium polarization
- detector calibration
- trigger commissioning

Already with the first data, a large number of $J/\psi \rightarrow \mu^+\mu^-$ and $\Upsilon \rightarrow \mu^+\mu^-$ decays are expected giving a unique opportunity for detector commissioning and alignment, calibration of the trigger and tracking systems, to test the QCD calculation based on earlier experiments and to study the main source of background for (rare) B processes. At already $60\ \mathrm{pn}^{-1}$ of collected data allow for a competitive measurement of the quarkonium polarization with enough statistics in the crucial high p_T region, where TEVATRON suffers form statistics. Even with $10\ \mathrm{pb}^{-1}$ ATLAS [25] will be able to measure ratios of quarkonia cross sections, which can help to constrain the non relativistic QCD Color Octet matrix elements.

When the LHC starts up in 2009/10, ATLAS and CMS will have unique opportunities to study beauty and charm production from pp collisions at $\geq 10\ \mathrm{TeV}$ making use of first data. In the initial phase of the LHC operation at lower luminosity several Standard Model physics analyses have to be performed to contribute to the commissioning and validation of the detector and trigger systems. The production of charmonium states will then be one of the key players in the early data taking. One of the initial measurements is the $B^+ \rightarrow J/\psi K^+$ channel, which will be an important reference channel for the search for di-muons from rare B decays and a control channel for the CP violation measurement used to estimate systematic uncertainties and tagging efficiencies at higher luminosities. Due to the huge $b\bar{b}$ cross-section and the expected high rates of the corresponding triggers, the data collection for beauty measurements can be done easily during the low luminosity phase.

Charmonium Production

Understanding the production of prompt quarkonia at the LHC is an important step to understand the underlying QCD mechanisms, and one that has given rise to controversy, both with respect to the cross-section magnitude and the polarization [28, 29]. The initial discrepancy in cross-section led to the Color Octet Model [27] but more high p_T results are needed to distinguish between this and competing models.

In addition to these open questions, the narrow J/ψ resonance is ideal for studies of detector performance. The expected abundant production (see Fig. 13) makes this feasible already in the very early data.

Both decay channels $J/\psi \rightarrow \mu^+\mu^-$ and $J/\psi \rightarrow e^+e^-$ will be used as tools to test our detector performance. In the following only the J/ψ resonance is considered. Quarkonia selection in ATLAS and CMS are mainly based on a di-muon trigger which requires two identified muons, both with $p_T \geq 4\ \mathrm{GeV}$ and within a pseudorapidity of $|\eta| < 2.4$.

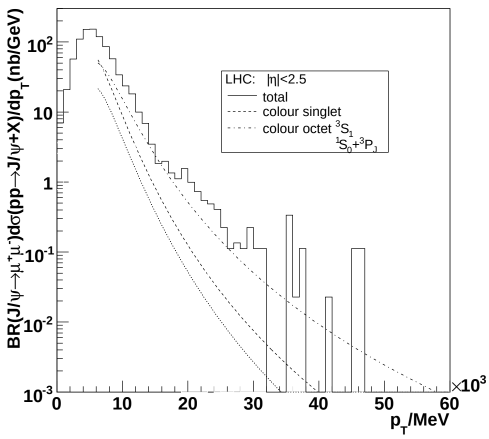

Figure 13: Differential J/ψ cross-sections as predicted from the Color Octet Model. Contributions from (singlet) χ production is included.

The di-muon sample considered here has offline p_T cuts of 6 and 4 GeV applied to the two identified muons. To suppress backgrounds (decays-in-flight, heavy flavor decays) tracks are required to come from the same vertex and with a pseudo-proper time cut of $\tau = 0.2$ ps, defined as $\tau = \frac{M \cdot L_{xy}}{p_T(J/\psi) \cdot c}$. In Fig. 14 the resulting di-muon spectrum with background contributions is shown. The mass resolution for $J/\psi \to \mu^+\mu^-$ is expected to be 53 MeV.

The possibility of doing performance measurements using di-electron resonances has also bees studied for ATLAS. In that case the E_T cut for both leptons is 5 GeV at trigger level and offline, and $|\eta| < 2$. Tight electron identification cuts are applied to reject background, including E/p, vertexing layer hit on the tracks, and the ratio of high to low threshold hits in the transition radiation tracker. The mass resolution for $J/\psi \to e^+e^-$ is expected to be about 200 MeV, see Fig. 14 richt. The width is mainly constrained by bremsstrahlung due to the large amount of material in the inner detector.

Charmonium Polarization

In addition to cross-section measurements ATLAS and CMS will use the quarkonia di-muon decays to provide answers to the polarization puzzle and help constrain the models. Defining the polarization parameter α as $\alpha = (\sigma_T - 2\sigma_L)/(\sigma_T + 2\sigma_L)$, this can measured via θ^*, the angle between J/ψ in rest frame and μ^+, as they are related by:

$$\frac{dN}{d\cos\theta^*} = C \cdot \frac{3}{2\alpha + 6} \cdot (1 + \alpha \cos^2\theta^*) \qquad (15)$$

With the di-muon triggers a rather narrow $\cos\theta^*$ distribution can be get, with both muons having similar p_T. To access higher values of $\cos\theta^*$ a single muon trigger is used where the trigger muon can be paird with a low p_T track to get large Δp_T and $\cos\theta^*$. For the result from ATLAS quoted here, a trigger threshold of 10 GeV is used for the single muon trigger and the p_T requirement on the second track was 0.5 GeV. The looser cuts allow for more background but still with decent signal to background discrimination ($S/B = 1.2$ for J/ψ). This dataset was added (with corrections for overlaps) to complement the di-muon triggered dataset. The combined $\cos\theta^*$ distributions were then fitted for α and C in slices of p_T. The tests have been carried out with unpolarized samples and with $\alpha = \pm 1$.

A measurement of the J/ψ polarization with the p_T of the J/ψ in the range of 10 GeV (trigger dependent) up to 50 GeV can be expected. Already with the first 10 pb^{-1} a better precision than the current Tevatron measurements can be achieved - but with J/ψ at high p_T, which is what is needed to truly distinguish between models.

Conclusions

It could be shown in this proceedings, that charm production is still a big issue at many experiments of HERA and TEVATRON and their results will have a large inpact to the LHC experiments. Charm physics is still a very active field on hadron colliders delivering inportant insights for theoretical predictions. Fundamental inputs from the HERA experiments H1 and ZEUS to the charm contributions to the proton structure functions have been presentet as well the measurement of the charm fragmentation function. Results of charmonium production in media have been shown form HERA-B. Furthermore, important results form TEVATRON on measurements flavour changing currents and associated W with charm-jet production have been discussed. Also measurement of charmonium production, spectroscopy and polarzation were done at TEVATRON but could not be discussed here.

All this measurements are fundamental inputs for the interpretation of the results from LHC. On one hand, a good knowlede of the charm contribution to the proton structure function is inevitable. On the other hand, charmonium states are well known standard model processes to be used to understand and calibrate the detector and for trigger commissioning. Furthermore, charmonium production is important for many searches of rare B decay exporing the indirects effects of new physics. The experiment $LHCb$ is expected to give also many new inputs to charm physics.

References

[1] H1-Collaboration, arXiv:0907.2643v2 [hep-ex], accepted by Eur.Phys.J.

[2] ZEUS-Collaboration, Eur.Phys.J.C(2010)65.

[3] E. Laenen *et al.*, Phys.Lett.B291(1992)325;
E. Laenen *et al.*, Nucl.Phys.B392(1993)162,229;
S. Riemersma, J. Smith and W.L. van Neerven, Phys.Lett.B347(1995)143;
B.W. Harris and J. Smith, Phys.Rev.D57(1998)2806.

[4] G. Watt, A.D. Martin, W.J.Stirling, R.S. Thorne, [arXiv:0806.4890].

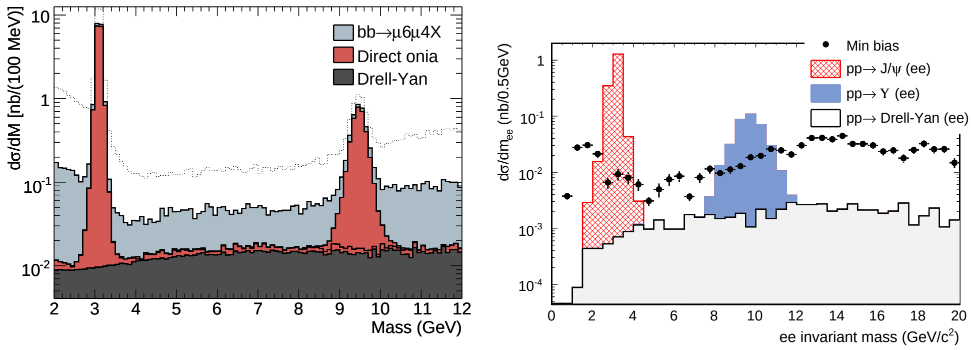

Figure 14: Di-lepton mass distributions for muons (left) and electrons (right) from ATLAS. In the left plot the spectrum in case of no vertex cuts (top dashed line) is also shown.

[5] H1-Collaboration, arXiv:0904.0929

[6] H1-Collaboration, Eur.Phys.J.C59 (2009) 589.

[7] ZEUS-Collaboration, J. High Energy Phys.04(2009)082.

[8] R. Vogt, Phys.Ref.C61(2000)035203;
R. Vogt, Phys.Ref.C71(2005)054902.

[9] M.J. Leitch *et al.*, Phys.Rev.Lett.84(2000)3256.

[10] NA50-Collaboration, Eur.Phys.J33(2004)31;
C. Lourenço, Nucl.Phys.A783(2007)451.

[11] M. Hirai, S. Kumano and T. H. Nagai, Phys.Rev.C70(2004)044905.

[12] K.J. Eskola, V.J. Kolhinen and C.A. Salgado, Eur.Phys.J9(1999)61.

[13] K. J. Eskola, V. J. Kolhinen and P. V. Ruuskanen, Nucl.Phys.B535(1998)351.

[14] S. Gavin and J. Milana, Phys.Ref.Lett.68(1992)1834;
S. Brodsky and P. Hoyer, Phys.Lett.B298(1993)165.

[15] HERA-B-Collaboration, Phys.Lett.B638(2006)407.

[16] HERA-B-Collaboration, Eur.Phys.J.C60(2009)525.

[17] E789-Collaboration, Phys.Rev.Lett.72(1994)1318;
E789-Collaboration, Phys.Rev.D52(1995)1307;
E771-Collaboration, Phys.Rev.D55(1997)3927;
E672/706-Collaboration, Phys.Rev.D62(2001)012001-1.

[18] R.J. Glauber and M. Matthiae, Nucl.Phys.B21(1970)135.

[19] K. J. Eskola, H. Paukkunen and C. A. Salgado, arXiv:0802.0139 [hep-ph].

[20] HERA-B-Collaboration, Phys.Rev.D79(2009)012001.

[21] CDF-Collaboration, Phys.Rev.Lett.100(2008)091803.

[22] D0-Collaboration, Phys. Lett.B666(2008)23.

[23] HERA-B-Collaboration, Phys.Lett.B596(2004)173.

[24] CDF-Collaboration, Phys.Rev.D68(2003)091101.

[25] ATLAS-Collaboration, JINST 3:S08003,2008.

[26] CMS-Collaboration, CMS PAS BPH-07-002.

[27] G. Bodwin, E. Braaten, and G. Lepage, Phys.Rev.D51(1995)1125.

[28] CDF-Collaboration, Phys.Rev.Lett.69(1992)3704;
Phys.Rev.Lett.99(2007)132001 (2007).

[29] D0-Collaboration, arXiv:0804.2799 (2008).